# Combined Contactless Conductometric, Photometric, and Fluorimetric Single Point Detector for Capillary Separation Methods

**ARTICLE** *in* ANALYTICAL CHEMISTRY · DECEMBER 2009

Impact Factor: 5.64 · DOI: 10.1021/ac902376v · Source: PubMed



**7 AUTHORS**, INCLUDING:

Frantisek Foret
Institute of Analytical Chemistry, CAS, Brn…
**177** PUBLICATIONS **5,289** CITATIONS
SEE PROFILE

Peter C Hauser
University of Basel
**206** PUBLICATIONS **5,730** CITATIONS
SEE PROFILE

Brett Paull
University of Tasmania
**242** PUBLICATIONS **3,095** CITATIONS
SEE PROFILE

Miroslav (Mirek) Macka
University of Tasmania
**215** PUBLICATIONS **4,021** CITATIONS
SEE PROFILE

*Anal. Chem.* **2010,** *82,* 129–135

# Combined Contactless Conductometric, Photometric, and Fluorimetric Single Point Detector for Capillary Separation Methods

**Markéta Ryvolová,[†,‡] Jan Preisler,[‡] František Foret,[§] Peter C. Hauser,[∥] Pavel Krásenský,[‡] Brett Paull,[†] and Mirek Macka*[,†]**

*Irish Separation Science Cluster and National Centre for Sensor Research, Dublin City University, Dublin, Ireland, Department of Chemistry and Department of Experimental Biology, Faculty of Science, Masaryk University, Kotlářská 2, 61137 Brno, Czech Republic, Institute of Analytical Chemistry of the ASCR, v.v.i., Veveří 97, 60200 Brno, Czech Republic, and Department of Chemistry, University of Basel, 4056 Basel, Switzerland*

**This work for the first time combines three on-capillary detection methods, namely, capacitively coupled contactless conductometric ($C^4D$), photometric (PD), and fluorimetric (FD), in a single (identical) point of detection cell, allowing concurrent measurements at a single point of detection for use in capillary electrophoresis, capillary electrochromatography, and capillary/nanoliquid chromatography. The novel design is based on a standard 6.3 mm i.d. fiber-optic SMA adapter with a drilled opening for the separation capillary to go through, to which two concentrically positioned $C^4D$ detection electrodes with a detection gap of 7 mm were added on each side acting simultaneously as capillary guides. The optical fibers in the SMA adapter were used for the photometric signal (absorbance), and another optical fiber at a 45° angle to the capillary was applied to collect the emitted light for FD. Light emitting diodes (255 and 470 nm) were used as light sources for the PD and FD detection modes. LOD values were determined under flow-injection conditions to exclude any stacking effects: For the 470 nm LED limits of detection (LODs) for FD and PD were for fluorescein ($1 \times 10^{-8}$ mol/L) and tartrazine ($6 \times 10^{-6}$ mol/L), respectively, and the LOD for the $C^4D$ was for magnesium chloride ($5 \times 10^{-7}$ mol/L). The advantage of the three different detection signals in a single point is demonstrated in capillary electrophoresis using model mixtures and samples including a mixture of fluorescent and nonfluorescent dyes and common ions, underivatized amino acids, and a fluorescently labeled digest of bovine serum albumin.**

Capillary separation techniques including capillary/nanoliquid chromatography (capillary/nano-LC), capillary electrochromatography (CEC), and capillary electrophoresis (CE) are key analytical techniques in many modern areas of science, including proteomics, pharmaceutical, biological, biochemical, medical, forensic, environmental, and other applications. Because of the complexity of real samples, the choice of the optimal detection mode can be problematic. Currently most common methods used for on-capillary detection in separations are photometric (PD),[1−3] fluorimetric (FD),[4−6] and conductometric detectors, the later mostly realized in the capacitively coupled contactless conductometric ($C^4D$) mode.[7−10] Each of these techniques is strongly dependent on the properties of studied analytes, and none of them are both truly universal and highly sensitive. These individual detection modes in CE have been reviewed recently.[8,11−13] Nowadays mass spectrometric (MS) detection should be included in the group of popular detection methods in capillary separations, and while about an order of magnitude more costly, it provides a means of positive identification of analytes and can be coupled to follow after the contactless noninvasive methods of PD, FD, and $C^4D$.[14]

Simultaneous detection of compounds with different properties present in complex samples is desirable but often quite challenging. Because of the limitations of the above-mentioned commonly used detection techniques, combinations of these methods have been attracting an increasing interest. Simple connection of different individual detectors in series along the separation capillary has been used to increase the versatility of detection;[15−19] however, this arrangement brings problems to data evaluation due

* Corresponding author. Phone: +353-01-700-5611. E-mail: mirek.macka@gmail.com.
[†] Dublin City University.
[‡] Masaryk University.
[§] Institute of Analytical Chemistry of the ASCR v.v.i.
[∥] University of Basel.

(1) Johns, C.; Macka, M.; Haddad, P. R. *Electrophoresis* **2003**, *24*, 2150–2167.
(2) Otieno, A. C.; Mwongela, S. M. *Anal. Chim. Acta* **2008**, *624*, 163–174.
(3) Tůma, P.; Samcová, E. *Chem. Listy* **2007**, *101*, 200–207.
(4) Lacroix, M.; Poinsot, V.; Fournier, C.; Couderc, F. *Electrophoresis* **2005**, *26*, 2608–2621.
(5) Lin, Y. W.; Chiu, T. C.; Chang, H. T. *J. Chromatogr., B* **2003**, *793*, 37–48.
(6) Paez, X.; Hernandez, L. *Biopharm. Drug Dispos.* **2001**, *22*, 273–289.
(7) Guijt, R. M.; Evenhuis, C. J.; Macka, M.; Haddad, P. R. *Electrophoresis* **2004**, *25*, 4032–4057.
(8) Kubáň, P.; Hauser, P. C. *Electroanalysis* **2004**, *16*, 2009–2021.
(9) Šolínová, V.; Kašička, V. *J. Sep. Sci.* **2006**, *29*, 1743–1762.
(10) Kubáò, P.; Hauser, P. C. *Anal. Chim. Acta* **2008**, *607*, 15–29.
(11) Schulze, P.; Belder, D. *Anal. Bioanal. Chem.* **2009**, *393*, 515–525.
(12) Swinney, K.; Bornhop, D. J. *Electrophoresis* **2000**, *21*, 1239–1250.
(13) Wang, J. *Electroanalysis* **2005**, *17*, 1133–1140.
(14) Klampfl, C. W. *Electrophoresis* **2006**, *27*, 3–34.
(15) Agrafiotou, P.; Sotiropoulos, S.; Pappa-Louisi, A. *J. Sep. Sci.* **2009**, *32*, 949–954.
(16) Chang, P. L.; Lee, K. H.; Hu, C. C.; Chang, H. T. *Electrophoresis* **2007**, *28*, 1092–1099.
(17) Chicharro, M.; Bermejo, E.; Ongay, S.; Zapardiel, A. *Electroanalysis* **2008**, *20*, 534–541.

10.1021/ac902376v 
Published on Web 12/04/2009

to the migration time shift and peak broadening, therefore mathematical corrections are needed. To overcome this limitation, combined detectors with single (identical) point of detection (1-DP) have been suggested. So far, very few examples of 1-DP combined detectors have been presented, most of them combining two different modes of detection: photometric−fluorimetric,[20] photometric−conductivity,[21−23] and conductivity−fluorescence.[24] To the authors' best knowledge, only two of them ($C^4D$−FD and $C^4D$−PD) have been commercialized (CE Resources, Singapore).[25]

Simultaneous detection using three modes, namely, photometric, fluorimetric, and conductometric in one purpose designed HPLC detection cell has been presented by Schmidt and Scott in 1985.[26] It must be pointed out that in contrast to ref 26 based on the now superseded wet-style contact-mode conductivity detection (electrode in contact with the detected solution) that is known to be plagued by problems such as electrode fouling, the here presented detection design uses on-capillary contactless conductivity detection ($C^4D$), and also the rest of the detection assembly is completely different.

In this work, an original design of a 1-DP on-capillary 3-in-1 detector is presented combining three detection modes PD, FD, and $C^4D$ (here further termed "1-DP 3-in-1 detector") and demonstrated to achieve concurrent detection in a simple and effective way in CE with a clear potential for use in other capillary separation methods including CEC, nano-liquid chromatography (nano-LC), capillary isoelectric focusing (CIEF), etc. This new detection capability effectively tripling the detection information about the sample gained in a single separation run has the potential for the analysis of complex samples. As the three concurrent detection modes are noninvasive and nondestructive, the 1-DP 3-in-1 detector allows for further online coupling with an MS system.

## EXPERIMENTAL SECTION

**Chemicals, Materials, and Methods.** All reagents, *N*-cyclohexyl-2-aminoethanesulfonic acid (CHES) buffer, 2-(*N*-morpholino)ethanesulfonic acid (MES), tris(hydroxymethyl)aminomethane (TRIS), sodium phosphate, dithiothreitol (DTT), acetone, histidine, cysteine, *N*-acetyl cysteine, tryptophan, tyrosine, potassium chloride, fluorescein isothiocyante (FITC), bovine serum albumin (BSA), fluorescein, and tartrazine were of analytical grade purchased from Sigma Aldrich (Ireland). Trypsin was purchased from Fluka (Germany). Background electrolyte (BGE) solutions were prepared by dissolving the respective compound in ultrapure water (Millipore).

For LOD determination, solutions were further diluted with the BGE 1:100. The solution of fluorescein for FD characterization was prepared by dissolving in CHES buffer (20 mmol/L, pH 9) at the concentration of $5 \times 10^{-7}$ mol/L. Tartrazine test solution ($c = 1 \times 10^{-5}$ mol/L) for PD characterization was prepared by dissolving in sodium phosphate buffer (20 mmol/L, pH 11). LOD determinations were conducted in a flow injection mode.

Solutions of model compounds dissolved in BGE (CHES buffer, $c = 20$ mmol/L pH 9) were mixed to following concentrations: fluorescein $5 \times 10^{-6}$ mol/L, tartrazine $5 \times 10^{-4}$ mol/L, KCl $5 \times 10^{-3}$ mol/L, His $2.5 \times 10^{-3}$ mol/L, MES $2.5 \times 10^{-3}$ mol/L, Trp $3.7 \times 10^{-4}$ mol/L, Tyr $7.5 \times 10^{-4}$ mol/L, Cys $9.4 \times 10^{-4}$ mol/L, and NAC $5.6 \times 10^{-4}$ mol/L.

The FITC-labeled BSA digest was prepared according to the procedures described elsewhere.[27,28] Briefly, 250 $\mu$L of BSA (0.1 mg/mL) in TRIS buffer (10 mmol/L, pH 7.8) was mixed 30 $\mu$L of DTT (36 mg/mL) in TRIS buffer (10 mmol/L, pH 7.8) and heated for 1.5 h at 35 °C. A volume of 100 $\mu$L of the mixture was mixed with 100 $\mu$L of trypsin (1.3 mg/mL) in TRIS buffer (10 mmol/L, pH 7.8) and heated for 15 h at 35 °C. Subsequently, 100 $\mu$L of digest was mixed with 100 $\mu$L of FITC in acetone (5 mmol/L) and heated for 5 h at 50 °C. The mixture was diluted 1:10 with BGE (CHES buffer, 20 mmol/L, pH 9) prior to separation.

**Experimental Setup.** A portable CE setup described elsewhere[29−32] was used in this work. In laboratory conditions, an external HV supply (Electro Automatic, EA-PS 2016-050) was used as a power source.

Fused silica capillaries (Polymicro Technologies) of 75 $\mu$m i.d. and 375 $\mu$m o.d. were employed for all experiments in this work. The total length of the capillary was 39.0 cm, and the effective length to the detector was 31.5 cm. CE analyses in all cases were performed at a voltage of +15 kV, and the sample was injected hydrodynamically for 10 s by the height difference of 10 cm (1 kPa).

**Detector Setup.** The detector body was integrated and assembled onto a machined aluminum "detector assembly" disk of a 45 mm diameter and 6 mm thickness with a central hole (6.5 mm diameter), through which the SMA adapter (905/906, Amphenol) was mounted at 90° to the disk plane and which also served as an alignment platform for the tubes positioning the CE separation capillary and the FD excitation and emission optical fibers (OF) (Figure 1). A second aluminum "cover" disk of similar shape and size served merely as a cover once the cell has been assembled and aligned to provide mechanical robustness and Faradaic electrical shielding. The capillary passed through the center of SMA via holes (~0.4 mm) drilled in the walls of the SMA. On the surface of the detector assembly disk, orthogonally to the SMA the two metal tubes serving as both CE capillary alignment and $C^4D$ electrodes of inner diameter of 406 $\mu$m (critical), outer diameter approximately 600 $\mu$m (not critical), and length 10.0 mm were placed. The placement of the two separation capillary holder/$C^4D$ electrode tubes was precisely


(18) Chicharro, M.; Moreno, M.; Bermejo, E.; Ongay, S.; Zapardiel, A. *J. Chromatogr., A* **2005**, *1099*, 191–197.
(19) Tsukagoshi, K.; Sawanoi, K.; Nakajima, R. *J. Chromatogr., A* **2007**, *1143*, 288–290.
(20) Čáslavská, J.; Gassmann, E.; Thormann, W. *J. Chromatogr., A* **1995**, *709*, 147–156.
(21) Chvojka, T.; Jelínek, I.; Opekar, F.; Štulík, K. *Anal. Chim. Acta* **2001**, *433*, 13–21.
(22) Novotný, M.; Opekar, F.; Jelínek, I. *Chem. Listy* **2005**, *99*, 132–136.
(23) Novotný, M.; Opekar, F.; Jelínek, I.; Štulík, K. *Anal. Chim. Acta* **2004**, *525*, 17–21.
(24) Tan, F.; Yang, B. C.; Guan, Y. F. *Anal. Sci.* **2005**, *21*, 583–585.
(25) http://www.ce-resources.com/.
(26) Schmidt, G. J.; Scott, R. P. W. *Analyst* **1985**, *110*, 757–760.
(27) Encinar, J. R.; Ruzik, R.; Buchmann, W.; Tortajada, J.; Lobinski, R.; Szpunar, J. *Analyst* **2003**, *128*, 220–224.
(28) Takizawa, K.; Nakamura, H. *Anal. Sci.* **1998**, *14*, 925–928.
(29) Kappes, T.; Galliker, B.; Schwarz, M. A.; Hauser, P. C. *TrAC, Trends Anal. Chem.* **2001**, *20*, 133–139.
(30) Kappes, T.; Hauser, P. C. *Anal. Commun.* **1998**, *35*, 325–329.
(31) Kappes, T.; Schnierle, P.; Hauser, P. C. *Anal. Chim. Acta* **1999**, *393*, 77–82.
(32) Kubáň, P.; Nguyen, H. T. A.; Macka, M.; Haddad, P. R.; Hauser, P. C. *Electroanalysis* **2007**, *19*, 2059–2065.

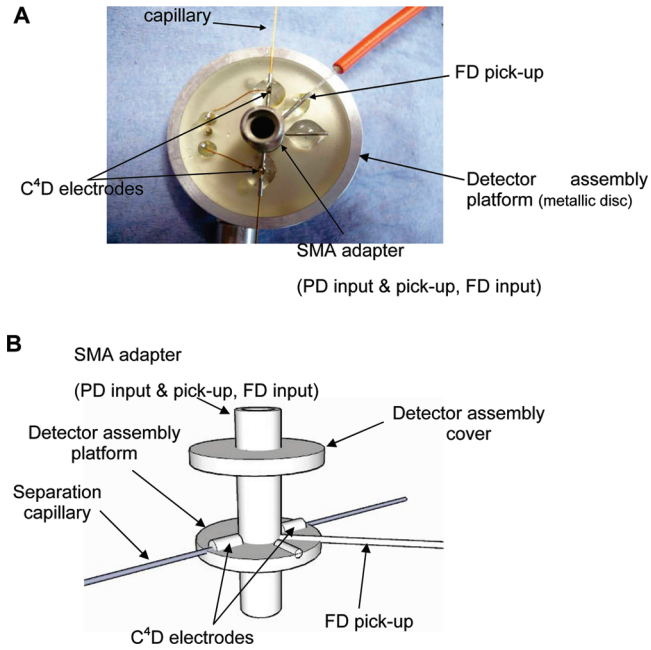


**Figure 1.** Depictions of the 3-in-1 detection cell: (A) photograph and (B) schematic drawing.

aligned using a magnifier lens to view light shining from the 50 $\mu$m i.d. OF through the separation capillary. The tubes were then affixed by gluing with two component epoxy glue (Patex, Henkel, Spain). This configuration facilitated easy capillary placement, replacement, and repositioning. The contactless conductivity detection cell was formed by the gap between these two electrodes, which were positioned just outside of the used SMA adapter. For the standard SMA adapter of 6.3 mm o.d., the electrode gap was 7.0 mm. The SMA walls at the same time served as a Faradaic shielding for the $C^4D$. To the excitation electrode, the high frequency electric field was connected and the second electrode served as an output. The capillary was fixed in certain position with tightening of two circle discs of the detector together.

Two light emitting diodes (LEDs) were used as light sources for PD and FD, 470 nm (B3B-447-IX, Roithner Lasertechnik, Austria) and 255 nm (T5F25C, SeoulOpto, South Korea). The 470 nm LED was powered with 30 mA, and the 255 nm LED was powered with 25 mA using laboratory-made constant current power supplies.

For PD, a 300 $\mu$m OF (Ocean Optics) was used to guide the light from the LED to one side of the detection cell (SMA), and another OF (50 $\mu$m, Ocean Optics) was utilized to guide the light from the cell (SMA) so the CE capillary passed between the incoming-light and transmitted-light OFs. A silicon photodiode with preamplifier (NT59-393, Edmund Optics, U.K.) was used as a detector for the 470 nm LED and a miniature photomultiplier tube (Hamamatsu, U.K.) for the 255 nm LED.

For FD, fluorescence emission was monitored by a second PMT (Hamamatsu, U.K.) connected to the OF (Polymicro Technologies, 300 $\mu$m) placed into the metal tube with inner diameter 406 $\mu$m. This tube was, similarly to the conductivity electrodes, placed on the surface of the detector disk. The angle between the capillary and the fluorescence output fiber was 45°. As with the PD detection alignment through the CE capillary center as described above, the OF and capillary position was adjusted under the magnifying lens by manipulating the fiber in the metal tube to be touching the capillary. A long pass filter $\lambda_c$ = 515 nm (Edmund Optics, U.K.) was inserted at the entrance of the PMT to block the excitation light and reduce the FD background noise.

In-house made $C^4D$ detector electronics described previously[32] were used. A high-frequency electric field was produced by a function generator (ISO-TECH GFG-8216A) coupled to the excitation electrode of the $C^4D$. A pick-up amplifier equipped with a feedback resistor of 1 MΩ was inserted between the detection cell and the main circuitry of the $C^4D$ detector, which was housed separately.

The three independent signals (PD, FD, $C^4D$) were recorded by an eDAQ (Australia) multichannel data acquisition station with chromatographic (eDAQ Chart) software allowing registration of the three signal traces.

## RESULTS AND DISCUSSION

**Detector Design.** Different possible approaches in combining different detection modes may be possible in order to create an on-capillary detection system.[20,21,23] While dual detection systems have been already described and the advantages of a 3-in-1 detector are very obvious, it is a nontrivial challenge to design a 3-in-1 detection cell combining FD, PD, and $C^4D$ modes in a single detection point. The approach we took in this project was to utilize the optical alignment capabilities of a standard OF adapter of the type "SMA" for a PD and, while placing it orthogonally onto a small mounting platform, build all the other functional components for FD and $C^4D$ such as the OF and CE capillary tubular holders and $C^4D$ electrodes onto this platform as depicted schematically in Figure 1B.

It should be pointed out that a precise aligning of OFs used for PD presents a challenge for the detector design. Although several OF-based optical detectors have been presented,[21,23,33] the aligning of the OFs with sufficient precision has always been problematic. The commercially available standardized SMA adapter offers high precision in fiber aligning, and this can serve as a suitable detection platform for the 3-in-1 detection cell.[34] Therefore, PD realized with a SMA adapter can be expected to be relatively straightforward as well as the FD alignment, although for both, their performance parameters will depend on details of the design and have to be experimentally determined. On the other hand, the $C^4D$ has never been investigated before in an arrangement as in this work with the active tubular electrodes outside of a tubular central grounded electrode.

**$C^4D$ Design and Characterization.** The well-known design of on-capillary $C^4D$ consists of two tubular electrodes and optionally a grounded thin metal foil is inserted in-between to eliminate the stray capacitance.[8,10,35] It is well established that the $C^4D$ signal quality (S/N) is determined by the following system characteristics: (a) geometry, the shape of the electrodes, the gap between them and their placement along the capillary, presence of Faradaic shielding and (b) electrical

(33) Lindberg, P.; Hanning, A.; Lindberg, T.; Roeraade, J. *J. Chromatogr., A* **1998**, *809*, 181–189.
(34) Foret, F.; Zhou, H. H.; Gangl, E.; Karger, B. L. *Electrophoresis* **2000**, *21*, 1363–1371.
(35) Kubáň, P.; Hauser, P. C. *Electrophoresis* **2009**, *30*, 176–188.

**Table 1. Analytical Characteristics (LOD, RSD, Linear Range, and $r^2$) for Each Detection Method of 3-in-1 Detector[a]**

| detection method | analyte | LOD (mol/L) | peak height RSD (%) | retention time RSD (%) | linear range (mol/L) | $r^2$ |
|---|---|---|---|---|---|---|
| PD | tartrazine | $6 \times 10^{-6}$ | 6.9 | 1.9 | $1 \times 10^{-2}$ | 0.9858 |
| FD | fluorescein | $1 \times 10^{-8}$ | 5.3 | 1.2 | $1 \times 10^{-3}$[b] | 0.9917 |
| $C^4D$ | $MgCl_2$ | $5 \times 10^{-7}$ | 5.6 | 0.2 | $1 \times 10^{-3}$ | 0.9950 |

[a] Conditions: see Experimental Section. [b] The upper concentration range for which the $r^2$ is calculated. The absolute upper range cannot be determined for instrumental reasons (permanent damage of PMT).

parameters, the excitation voltage (primarily the amplitude and the frequency). The significant difference in this novel 3-in-1 detection cell design is the tubular SMA adapter placed in between the electrodes used to create the Faradaic shielding. As in this work, the geometry of the setup resulting from the optical SMA adapter is different from established designs, the electrical parameters necessary for an optimal $C^4D$ detection performance required optimization.

The optimal working frequency as a key factor for the conductivity detection was determined from the Bode plots.[36,37] The plots were constructed by manually controlling the input frequency applied on the excitation electrode from the function generator and recorded peak-to-peak amplitude being displayed numerically by the oscilloscope. The Bode plots were measured for an empty (dry) capillary and for a capillary filled with selected buffers to establish a comparison for the behavior of the cell for high- and low-conductivity buffers. As examples of typical low-conductivity buffers, MES/His (10, 20, 50 mmol/L, pH 6) and CHES (20 mmol/L, pH 9) were chosen. Sodium phosphate (20 mmol/L, pH 11) was tested as an example of a high-conductivity buffer. The frequency range chosen for construction of Bode plots was varied from 30 Hz to 1 MHz and the results plotted as signal, noise, and S/N ratio vs frequency (results not shown). As expected, the highest peak-to-peak amplitudes were gained for phosphate buffer; however, because of the relatively high noise levels in this buffer, overall the low conductivity buffers were preferred for the best results in terms of S/N values. From the Bode plots obtained for MES/His buffer in different concentration, the optimal results were achieved for 50 mmol/L solution. Consequently, S/N dependence on frequency in analysis of a 1 mmol/L KCl solution was plotted for these MES/His concentrations (10, 20, 50 mmol/L). From those data (not shown), the highest S/N ratio was obtained for 20 mmol/L MES/His buffer at a frequency of 50 kHz and therefore these conditions were used in further experiments.

Quantitative characterization of the $C^4D$ cell operated within a CE system for linearity and LOD was first performed using $K^+$ and $Mg^{2+}$ as a model ions. Excellent detection linearity characterized by a correlation coefficient of $R^2 = 0.9999$ over 4 orders of magnitude was determined. The LOD values determined for $K^+$ and $Mg^{2+}$ were $6.4 \times 10^{-6}$ and $5 \times 10^{-6}$ mol/L, respectively. A comparison of the obtained LODs in CE-mode with the best literature values[38] show about an order of magnitude higher LODs; however, comparisons in the CE mode may be easily distorted because of possible different stacking effects in different reports, and in fact our LOD values were obtained by injecting samples in the BGE that is under nonstacking conditions. Therefore, LOD values were also determined the same as for PD and FD in the flow-injection mode, and the summary of performance parameters is provided in Table 1. It should be also pointed out that currently the understanding of the role of the $C^4D$ detector geometry in its performance is still very limited and there is no general approach based on first principles allowing to design an optimal $C^4D$ detector; however, once the $C^4D$ design will be possible to approach using a model based on first principles by numerical simulations using a commercial software package, further advances in design and performance can be expected but such aims are clearly beyond the scope of this work. Importantly, the comparison of peaks shapes for those analytes that give detection response at both $C^4D$ and PD such as tartrazine (Figure 2) proved that the design with the two electrodes at a detection gap of ~7 mm, which is somewhat larger than typically used previously, does not produce any noticeable additional zone broadening.

**PD Design and Characterization.** PD is one of the most common and well established detection techniques that has been described in the literature in many different arrangements.[39−42] OF-based PD setups have become very popular through the past decade.[21,23,33,43] A crucial factor for a successful detector design and satisfactory performance for any miniaturized systems including on-capillary detection is accurate geometry and optical fiber-capillary alignment. Therefore the design of this new 3-in-1 PD detection cell was based on the SMA OF connector, the geometry of which allowed a highly accurate alignment of the two optical fibers. An accurate concentric alignment with the separation fused silica capillary is achieved through carefully positioning the $C^4D$ tubular electrodes acting as capillary guides using a microscope as described earlier.

Testing of PD designs is well established. The principle of photometric detectors characterization using sensitivity curves has been introduced by Cassidy and Janoski in 1992[44] and in a modified form subsequently by Macka and co-workers in a number of CE works as an objectively definable evaluation of detection linearity, effective path length in photometric detection, and the percentage of stray light.[45,46] Briefly, a sensitivity (defined


(36) Gillespie, E.; Connolly, D.; Macka, M.; Hauser, P.; Paull, B. *Analyst* **2008**, *133*, 1104–1110.
(37) Kubáň, P.; Hauser, P. C. *Electrophoresis* **2004**, *25*, 3398–3405.
(38) Kubáň, P.; Evenhuis, C. J.; Macka, M.; Haddad, P. R.; Hauser, P. C. *Electroanalysis* **2006**, *18*, 1289–1296.
(39) Cao, X. D.; Fang, Q.; Fang, Z. L. *Anal. Chim. Acta* **2004**, *513*, 473–479.
(40) Lim, K.; Kim, S.; Hahn, J. H. *Bull. Korean Chem. Soc.* **2002**, *23*, 295–300.
(41) Ro, K. W.; Lim, K.; Shim, B. C.; Hahn, J. H. *Anal. Chem.* **2005**, *77*, 5160–5166.
(42) Zhou, Z.; Wang, K. M.; Yang, X. H.; Huang, S. S.; Zhou, L. J.; Qin, D. L.; Du, L. *Analyst* **2001**, *126*, 1838–1840.
(43) Butler, P. A. G.; Mills, B.; Hauser, P. C. *Analyst* **1997**, *122*, 949–953.
(44) Cassidy, R.; Janoski, M. *LC GC Eur.* **1992**, *10*, 692.
(45) Johns, C.; Macka, M.; Haddad, P. R.; King, M.; Paull, B. *J. Chromatogr., A* **2001**, *927*, 237–241.

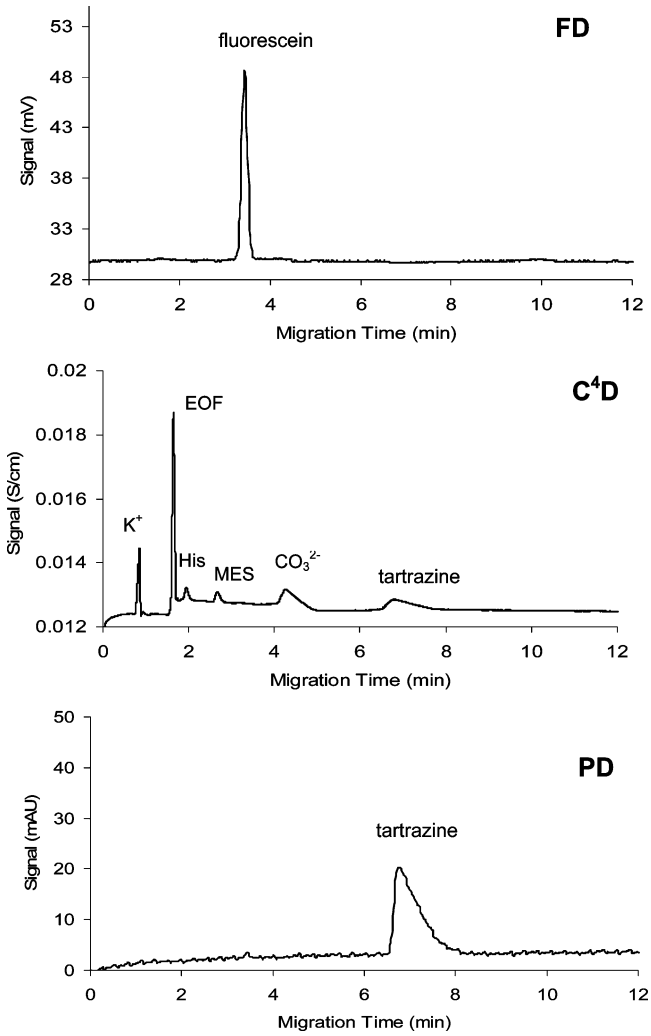


**Figure 2.** Separations of model mixtures with 3-in-1 detection. Conditions: electrolyte, 20 mmol/L CHES pH 9; PD, LED 470 nm; $C^4D$, frequency, 100 kHz; voltage, + 15 kV; injection, 10 s, 1 kPa; capillary, 75 $\mu$m, $l_{eff}$ = 31.5 cm; fluorescein 5 × $10^{-6}$ mol/L; tartrazine 5 × $10^{-4}$ mol/L; KCl 5 × $10^{-3}$ mol/L; His 2.5 × $10^{-3}$ mol/L; MES 2.5 × $10^{-3}$ mol/L.

as absorbance/concentration, $s = A/c$) vs absorbance graph is constructed. The percentage of stray light is calculated from the extrapolated maximum absorbance at the high-end of this sensitivity curve, and an effective path length is calculated at the low-end of this sensitivity curve from the sensitivity extrapolated to $A = 0$ using the Lambert−Beer law, namely, effective path length = sensitivity/absorbing compound absorptivity ($l_{eff} = s/\varepsilon$).

In this work, tartrazine ($\varepsilon$ = 21 600 L $mol^{-1}$ $cm^{-1}$) dissolved in phosphate buffer (20 mmol/L, pH = 11) was used as the test compound, and the calculated values for the percentage of stray light and effective path length for a 75 $\mu$m i.d. capillary were 11.5−21.2% and 37.0−41.2 $\mu$m, respectively, showing an acceptable performance. The effective path length lower than the highest possible maximum given by the capillary diameter is the result of "averaging" of the many present individual rays, most of them not passing through the center of the capillary. It has to be noted that a very precise alignment of the capillary (75 $\mu$m i.d. and 375 $\mu$m o.d.) using metal tubes of 406 $\mu$m i.d. to the center of the transmitted-light collecting OF (50 $\mu$m diameter) is required The somewhat high percentage of the stray light may be further improved by adjusting the position of the absorbance transmitted-light collecting OF to the optimal distance from the capillary (the further the OF is from the capillary, the lower the amount of stray light that can enter the transmitted-light collecting OF and reach the detector).

Practically the most important performance value for use in on-capillary detection in CE and other capillary separation methods is the baseline noise, directly affecting the LOD values: typical baseline noise values determined were in the range of 0.08 mAU (LED 470 nm). In this case of tartrazine, the S/N ratio for $C^4D$ is marginally better compared to PD and demonstrates that $C^4D$ is a relatively sensitive detection method, even compared to PD of highly absorbing species such as tartrazine in a well performing PD detection system. It is worth noting that since the LEDs are generally considerably less noisy than typical discharge lamps used in spectrophotometers, good sensitivity was achieved in spite of the single beam arrangement.

**FD Design and Characterization.** Even though the FD is the most sensitive detection method, where LODs can reach even single molecule level,[47] it is surprisingly also relatively the least technically demanding of the three, as no micrometer-precision fiber alignment is needed and generally the accuracy of the emission light collection fiber positioning in a tubular fiber guide properly positioned through the detector design is satisfactory. Therefore the most important condition in the detector design determining its performance is the general requirement of minimizing the excitation light reaching the PMT detecting the fluorescence emission. However, to fulfill this condition the application of optical filters has much higher importance than a precise positioning of the OFs. For these reasons, FD employing OFs is a highly popular configuration in fluorescence detectors employing lasers[48] as well as LEDs.[49,50]

The LOD value for a test analyte is the primarily important parameter characterizing the performance of FD. In this work, a regular 3 mm LED with the wavelength of 470 nm and optical power of 2.7 mW was used as a light source. Because of the losses at the LED coupling into the OF, the optical power of the excitation light at the end of the OF was only 22 $\mu$W as measured by a hand-held power meter (Edmund Optics, U.K.). Fluorescein was selected as the test compound with optimal spectral properties for the FD characterization.

**CE Separations.** The versatility of the 3-in-1 detector in terms of application to a standard separation method, as well as the possibility of the utilization of each detection mode separately or in any possible combination, gives the cell an unmatched advantage over detectors presented so far. CE has been chosen as a separation technique to demonstrate the 3-in-1 detector performance and illustrate its application potential. The applicability of the 3-in-1 detector for the analysis of complex mixtures containing analytes with different physical chemical properties was demonstrated using several samples and model mixtures of analytes possessing very different detection properties.

(46) Macka, M.; Andersson, P.; Haddad, P. R. *Electrophoresis* **1996**, *17*, 1898–1905.
(47) Chen, D. Y.; Dovichi, N. J. *Anal. Chem.* **1996**, *68*, 690–696.
(48) Taylor, J. A.; Yeung, E. S. *Anal. Chem.* **1992**, *64*, 1741–1744.
(49) Yang, B. C.; Guan, Y. F. *Talanta* **2003**, *59*, 509–514.
(50) Zhao, S. L.; Yuan, H. Y.; Xiao, D. *Electrophoresis* **2006**, *27*, 461–467.

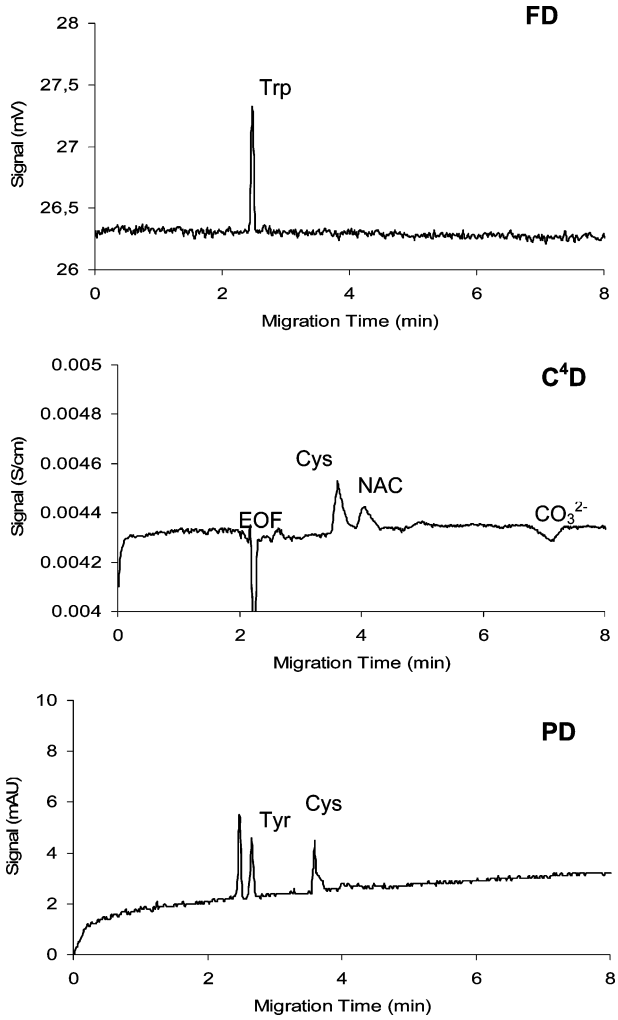


**Figure 3.** Separation of model mixture of amino acids. Conditions: Trp $3.7 \times 10^{-4}$ mol/L, Tyr $7.5 \times 10^{-4}$ mol/L, Cys $9.4 \times 10^{-4}$ mol/L, NAC $5.6 \times 10^{-4}$ mol/L separated in 20 mmol/L CHES pH 9; LED 255 nm; frequency, 100 kHz; voltage, + 15 kV; injection, 10 s, 1 kPa; capillary, 75 $\mu$m, $l_{eff} = 31.5$ cm.

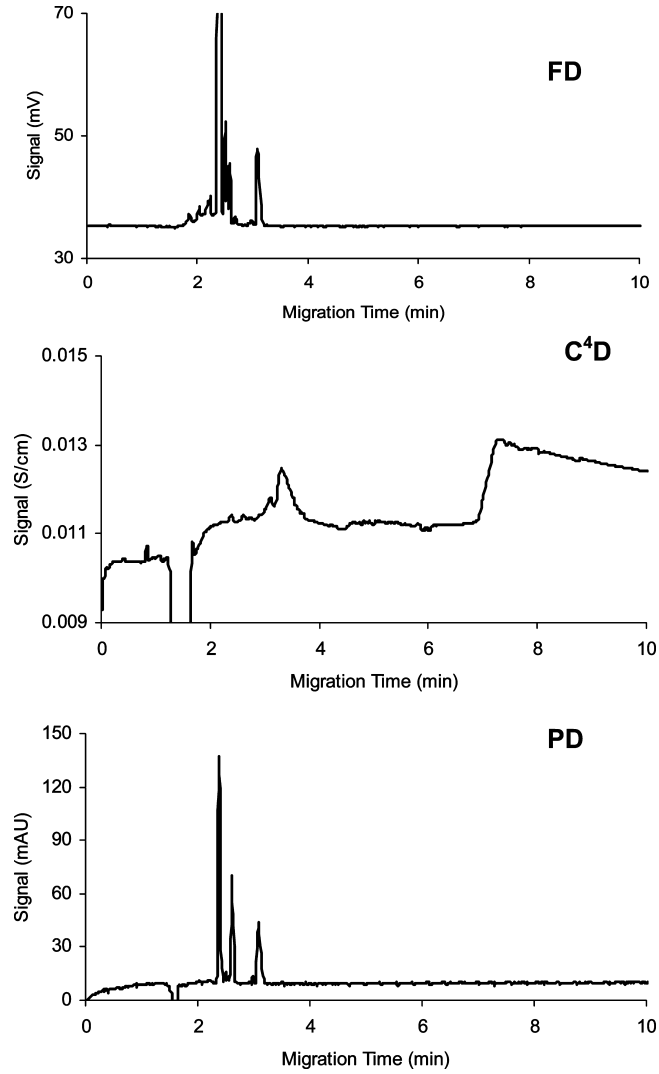


**Figure 4.** Separation of FITC-BSA digests components, for digestion and labeling conditions see the Experimental Section. Separated in 20 mmol/L CHES pH 9; LED 470 nm; frequency, 100 kHz; voltage, + 15 kV; injection, 10 s, 1 kPa; capillary, 75 $\mu$m, $l_{eff} = 31.5$ cm.

In the first example, the electopherograms for a separation of a model mixture of fluorescein, tartrazine, MES, His, and potassium chloride is shown in Figure 2. The carbonate peak present in the electropherogram is caused by absorption of the $CO_2$ in the air in the BGE. As expected, based on known detection properties of the model analytes, the three individual detection traces show corresponding responses. In the cases of all the presented electropherograms, they were repeatable and the baselines in all detection modes in absence of injected sample were free of any substantial fluctuations. The reproducibility of migration times and other performance characteristics are given in Table 1. The second example illustrates how a fiber-coupled LED as a light source enables an easy variability of excitation wavelengths according to the spectral properties of the analyte. A 255 nm UV-LED (with 100−150 $\mu$W optical power given by manufacturer) was used as an excitation source for simultaneous detection of four native (nonlabeled) amino acids with different detection properties in one separation run (Figure 3). The native fluorescence of tryptophan ($3.7 \times 10^{-4}$ mol/L) was detected, and the absorbance of tyrosine ($7.5 \times 10^{-4}$ mol/L) and tryptophan was measured while cysteine ($9.4 \times 10^{-4}$ mol/L) and *N*-acetylcysteine ($5.6 \times 10^{-4}$ mol/L) were determined conductometrically. The relatively high concentration of selected amino acids in the mixture was a result of the generally lower optical power of the LEDs in the UV spectral range compared to the vis-range LEDs.

The final example presented in Figure 4 shows a separation of a complex sample of FITC-labeled BSA digest. A variety of derivatized compounds is detected, and the advantage of the 3-in-1 detection is clearly demonstrated by the concurrent $C^4D$ detection of some nonlabeled components in the mixture, which were not detected by either FD or PD detection.

## CONCLUSIONS

The here developed 3-in-1 detection cell for the first time allows concurrent single point detection of three signals: contactless conductometric, photometric, and fluorimetric. The current design having the SME OF connector grounded and thus used as shielding in the $C^4D$ detection and the two electrodes with a detection gap of ~7 mm, which is somewhat larger than typically used previously, does not produce any noticeable

additional zone broadening. The design of the detector assembly is relatively simple and robust and further design changes may be possible that would bring improvements in detection performance of the three individual detectors. The possibility of moving the detection cell and using the $C^4D$ detection mode along the capillary fully remains in this design. The only additional requirement is associated with the optical detection modes PD and FD as would be expected, namely, the detection window in the polyimide coating or, alternatively, the use of a separation capillary with an optically transparent coating that would allow full axial translocation flexibility. The optical fiber-based FD detectors employing LEDs as a light source do not reach as low LODs as laser-based (LIF) detectors; however, the rapidly increasing optical power of LEDs available on the market promises improvements in detection sensitivity.

The detector offers a significant practical advantage of greater detection information while keeping one single point of detection, thus preserving identical times of peaks passing through the detector for the three different individual detection modes. CE was chosen as a separation technique for demonstration of the 3-in-1 performance, but it has to be emphasized that the applicability of the cell covers the whole range of on-capillary detection in microcolumn separations including CEC and nano-LC. For several model mixtures and samples it is demonstrated that the 3-in-1 combined detection enables single-run analysis of complex samples while providing more information about properties of the detected components.

The noninvasive, nondestructive contactless character of the 3-in-1 detection makes it also an ideal predetector for in-line coupled mass spectrometry analysis. This would be of great advantage especially for complex mixtures as can be clearly seen in the examples presented here and is one of the directions for further work in the area.

## ACKNOWLEDGMENT

The authors acknowledge the following sources of funding: Marie Curie Excellence Grants fellowship and Grant-MEXT-CT-2004-014361, The Ministry of Education, Youth and Sports of the Czech Republic Grant MSM0021622415, LC06023, the Czech Science Foundation Grant 203/09/1025, institutional grant of the AVCR AV0Z40310501, and Dr. Brian Lawless for technical help.

## NOTE ADDED AFTER ASAP PUBLICATION

This paper was published on the Web on December 4, 2009, with missing grant information in the Acknowledgment section. The corrected version was reposted on December 9, 2009.

Received for review July 3, 2009. Accepted November 15, 2009.

AC902376V